Supplement of Atmos. Chem. Phys., 22, 4705–4719, 2022
https://doi.org/10.5194/acp-22-4705-2022-supplement

Atmospheric Chemistry and Physics
Open Access

Supplement of

North China Plain as a hot spot of ozone pollution exacerbated by extreme high temperatures

Pinya Wang et al.

Correspondence to: Yang Yang (yang.yang@nuist.edu.cn)

Contents of this file

Text S1 to S3

Figures S1 to S7

Table S1 to S2

Text S1

Evaluation of OPCs simulated by GEOS-Chem during 2014-2017.

The GEOS-Chem simulated OPCs/OPIs during May-September 2014-2017 are identified using the same method described in Section 2 of the main text for observations. The spatial patterns of OPC and CF values of 2014-2017 are illustrated in Figure S4. The simulated OPC and CF spatial patterns are comparable to those of the observations, with higher values over the NCP region (37-41ºN; 114 -120ºE). The regional mean OPCs and CF values over NCP in observations are 19 days and 30%, respectively, while those in the GEOS-Chem simulation are 22 days and 35%. The spatial correlations between the simulated and observed OPCs and CF values are all higher than 0.5 and are statistically significant at 95% confidence level, accompanied by small mean bias (MB) and root mean square error (RMSE) values. For example, the MB between the simulated and observed OPCs and CF values over China are as low as 2.34 days and -0.23%, respectively. Moreover, the mean fractional bias (MFB) for CF values is well within the limit of MFB for O_3 evaluation (15%) recommended by EPA (2007). The statistical metrics suggest that the model can reasonably reproduce the observed spatial patterns and magnitudes of OPCs and CF over NCP during 2014-2017.

Text S2

Evaluation of OPCs in the CMIP6 simulations of present climate.

Here, the CMIP6 simulated OPCs are again identified using the same method described in Section 2. The spatial patterns of OPC and CF during 2015-2019 in observation and CMIP6 simulations under four SSPs are illustrated in Figure S6. The simulated OPCs and CF show similar spatial patterns compared to the observations, with higher values over the NCP regions (Figure S6). The regional mean OPC and CF over NCP (37-41ºN; 114 -120ºE) in the observations are 28 days and 37% respectively, during 2015-2019. The multi-model ensemble mean of CMIP6 simulations can reasonably reproduce the magnitudes of OPCs and CF values over NCP, with highest values under SSP2-4.5 (34 days & 44.5%) and lowest values under SSP3-7.0 (20.3 days &26.5%). Furthermore, the BIAS values between simulated and observed OPCs and CF values over China are the lowest under SSP3-7.0, as low as -2.37 days and -3.33%, respectively. Similarly, the MFB and RMSE for both simulated OPCs and CF values under SSP3-7.0 are the lowest among the four scenarios. The relatively higher MB and RMSE under SSP2-4.5 come from the overestimation of OPCs and CF values over the whole China, likely related to the inaccurate of SSPs emissions in China during this time period (Cheng et al., 2021; Wang et al., 2021).

Text S3

Method for mortality assessment.

The health impact function is widely applied to evaluate the mortality burden attributable to short-O3 and heat exposures.

$$\Delta Mort = BMR \times Pop \times (1 - 1/RR)$$

where ΔMort is the excess death due to O_3 exposure or heat exposure; BMR is the baseline daily mortality rate of the specific disease, and Pop is the population exposed to air pollution in different areas. RR represents the concentration/temperature-related relative risk of a specific disease caused by O_3/temperature exposures, which is calculated based on Eq. 6&7 in the main text. In this study, to obtain an estimation of daily excess death caused by increased ozone and temperature during OPCs than those during OPIs over NCP, the population and baseline mortality is collected from previous work (see Table S1 in Wang et al., 2021), using population and annual baseline mortality rate for the year of 2018 and assuming no significant changes in Pop (112.62 million) and BMR during 2014-2019. Note that the population in that study is for the Beijing–Tianjin–Hebei (BTH) region, and the baseline mortality rate are assumed evenly distributed across China as the city-level BMR is unavailable. T_0 and C_0 in Eq.6 &7 are set as 26°C and 0. In this study, the total excess mortality is assumed as the total excess deaths caused by increased O3 and temperatures. Based on the equation above, around 100 daily excess deaths are attributable to the higher temperatures and ozone level during OPCs ver NCP than OPIs.

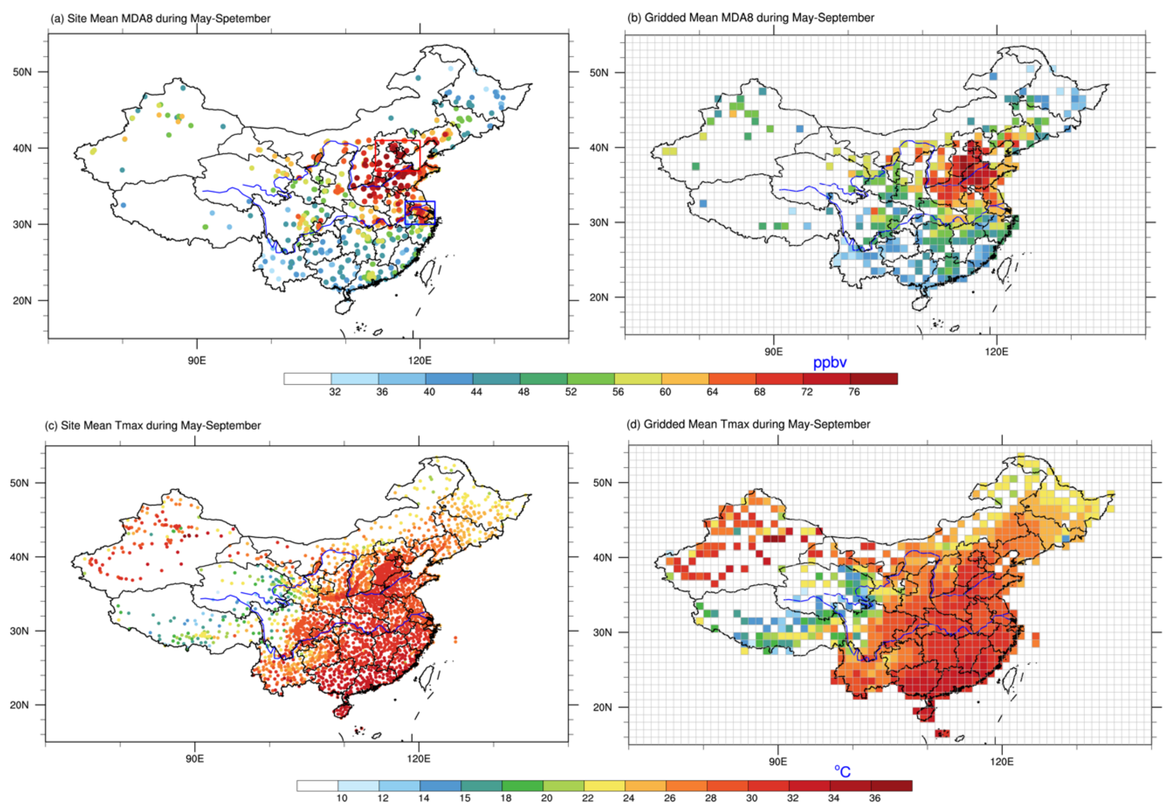

Figure S1. Spatial distributions of (a) site mean and (b) gridded mean MDA8 O_3, and (c) site mean and (d) gridded mean Tmax during May-September for 2014-2019. The red box and blue box in panel (a) represent the NCP region (37-41ºN; 114-120ºE) and the YRD region (30-33ºN; 118-120ºE), respectively.

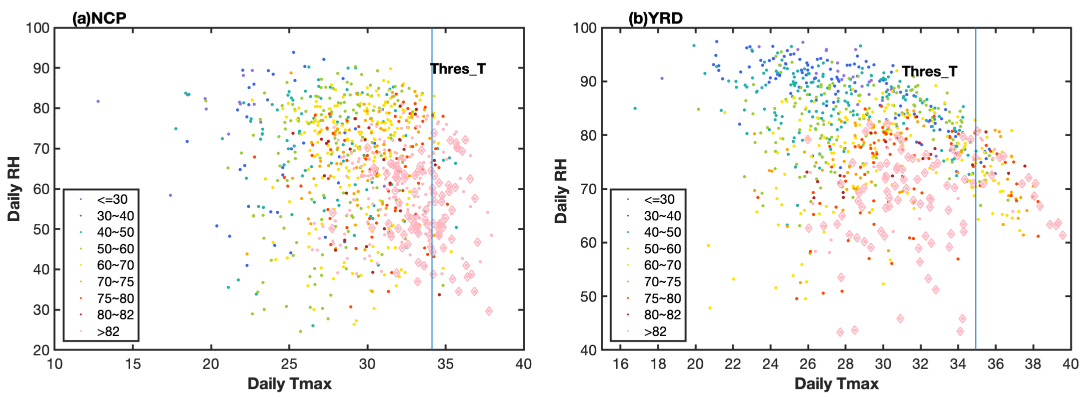

Figure S2. Daily MDA8 O_3 (ppbv, colored dots) as a function of the local daily Tmax and RH during May-September of 2014-2019 over (a) NCP (37-41°N; 114-120°E) and (b) YRD (30-33°N; 118-122°E). The larger pink squares denote the ozone pollution days with daily MDA8 O_3 exceeding the O_3 threshold. The vertical blue line denotes the threshold for extreme Tmax (Thres_T). Thus, the larger pink squares on the right side of the blue line represent coupled extreme days OPCs.

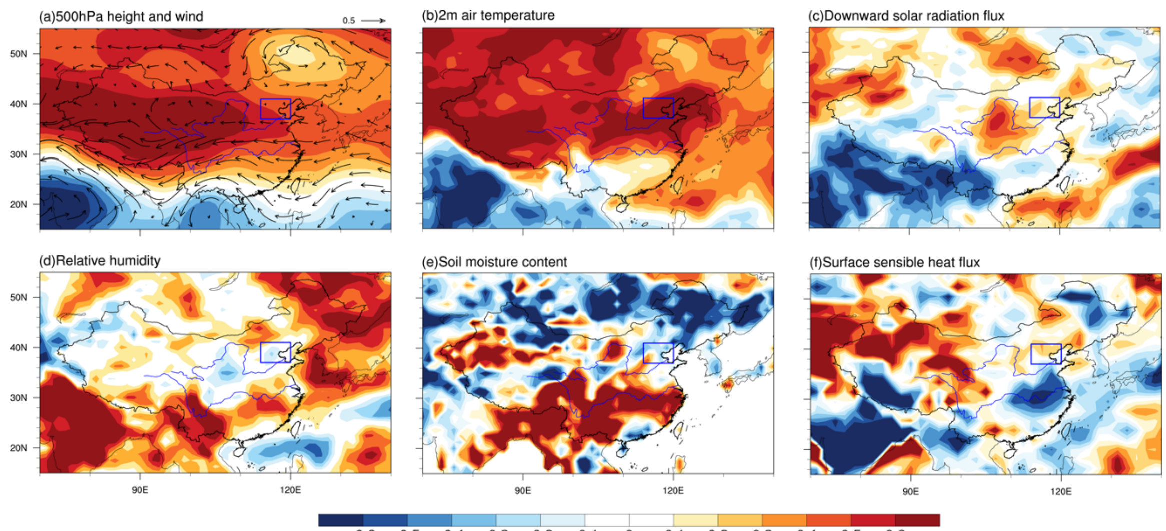

Figure S3. Differences between OPCs and OPIs (OPCs minus OPIs) composites of normalized anomalous (a) geopotential height and winds at 500hPa, (b) 2m air temperature, (c) downward solar radiation flux (DSR), (d) relative humidity, (e) soil moisture content, and (f) surface sensible heat flux. The blue box in each panel indicates the NCP region (37-41ºN; 114-120ºE).

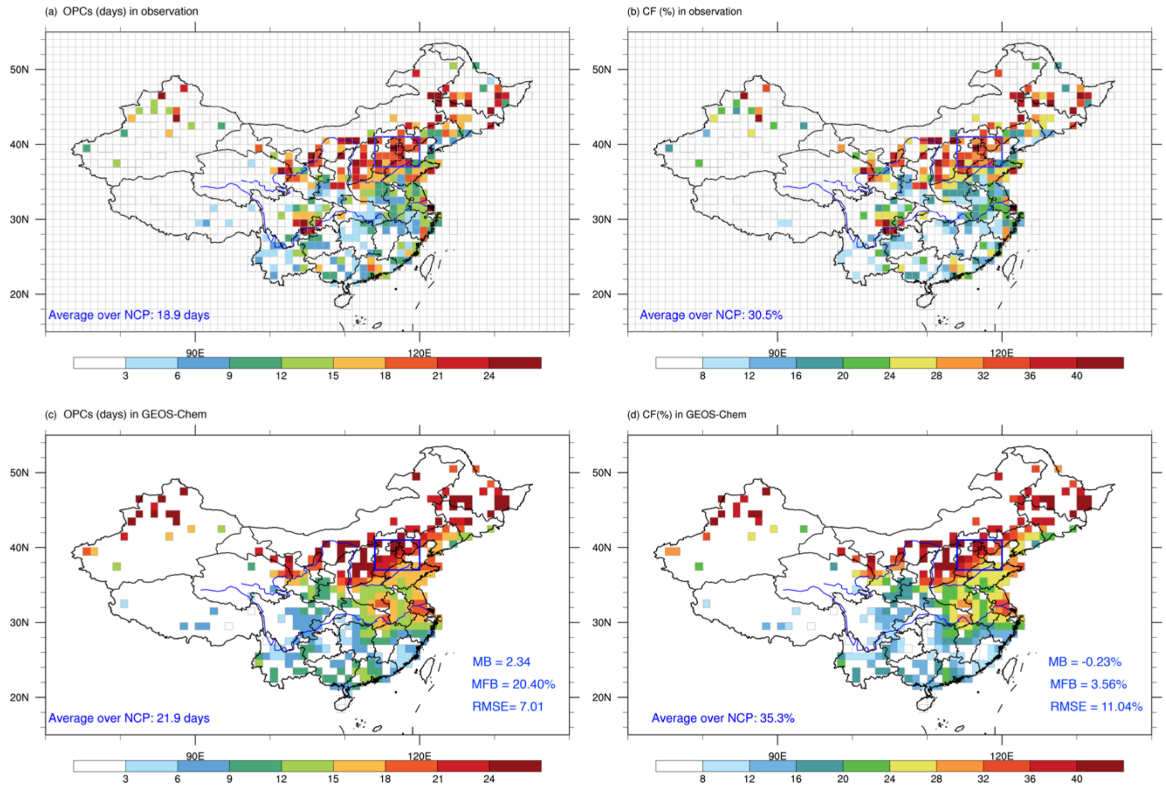

Figure S4. Spatial patterns of observed (a) OPCs (days) and (b) CF values (%) during May-September of 2014-2017. (c) and (d) are same as (a) and (b) but for the GEOS-Chem simulation. Observed and simulated values of OPCs(days) and CF averaged over NCP (37-41^{o}N; 114-120^{o}E) are indicated at the bottom left corner of each panel. Statistical metrics including MB, MFB, and RMSE are noted at the bottom right of panels (c) & (d). Note that the three metrics are obtained over the whole China, with equations listed in the appendix of Zhang et al. (2018).

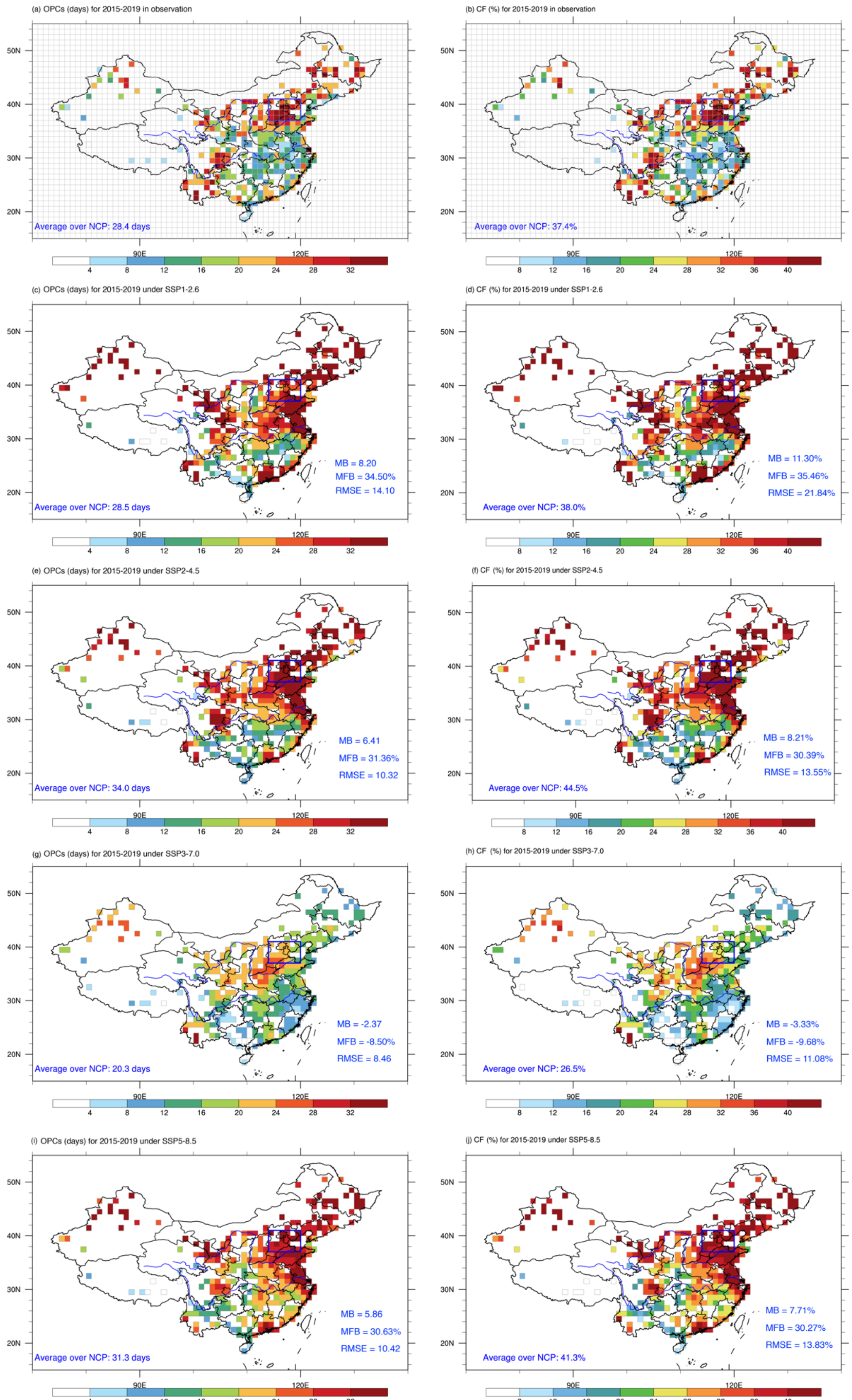
(a) OPCs (days) for 2015-2019 in observation
Average over NCP: 28.4 days
(b) CF (%) for 2015-2019 in observation
Average over NCP: 37.4%
(c) OPCs (days) for 2015-2019 under SSP1-2.6
MB = 8.20
MFB = 34.50%
RMSE = 14.10
Average over NCP: 28.5 days
(d) CF (%) for 2015-2019 under SSP1-2.6
MB = 11.30%
MFB = 35.46%
RMSE = 21.84%
Average over NCP: 38.0%
(e) OPCs (days) for 2015-2019 under SSP2-4.5
MB = 6.41
MFB = 31.36%
RMSE = 10.32
Average over NCP: 34.0 days
(f) CF (%) for 2015-2019 under SSP2-4.5
MB = 8.21%
MFB = 30.39%
RMSE = 13.55%
Average over NCP: 44.5%
(g) OPCs (days) for 2015-2019 under SSP3-7.0
MB = -2.37
MFB = -8.50%
RMSE = 8.46
Average over NCP: 20.3 days
(h) CF (%) for 2015-2019 under SSP3-7.0
MB = -3.33%
MFB = -9.68%
RMSE = 11.08%
Average over NCP: 26.5%
(i) OPCs (days) for 2015-2019 under SSP5-8.5
MB = 5.86
MFB = 30.63%
RMSE = 10.42
Average over NCP: 31.3 days
(j) CF (%) for 2015-2019 under SSP5-8.5
MB = 7.71%
MFB = 30.27%
RMSE = 13.83%
Average over NCP: 41.3%

Figure S5. Spatial patterns of (a) OPCs (days) and (b) CF values (%) during May-September of 2015-2019 in observation; (c)~(d), (e)~(f), (g)~(h), and (g)~(h) are same as (a) and (b) but for CMIP6 simulations under SSP1-2.6, SSP2-4.5, SSP3-7.0 and SSP5-8.5, respectively. OPCs (days) and CF averaged over NCP (37-41^{o}N; 114-120^{o}E) are indicated at the bottom left corner of each panel. Statistical metrics including MB, MFB, and RMSE are noted at the bottom right of panels (c)~(j). Note that the three metrics are obtained over the whole China.

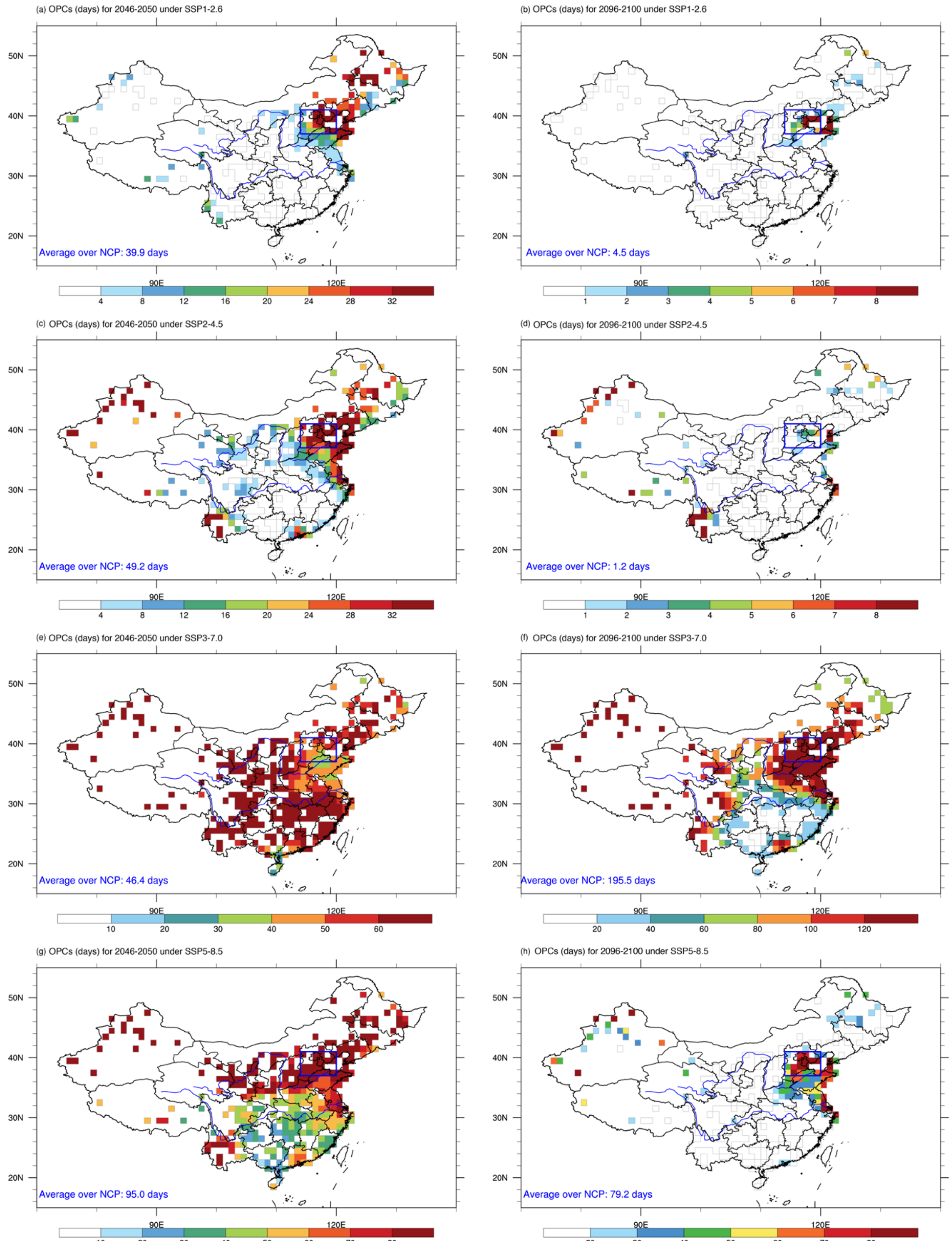

Figure S6. Spatial patterns of OPCs (days) during May-September in (a) 2046-2050 and (b) 2096-2100 under SSP1-2.6; (c)~(d), (e)~(f) and (g)~(h) are same as (a)~(b) but for simulations under

SSP2-4.5, SSP3-7.0 and SSP5-8.5, respectively. OPCs averaged over NCP (37-41ºN; 114-120ºE) are indicated at the bottom left corner of each panel.

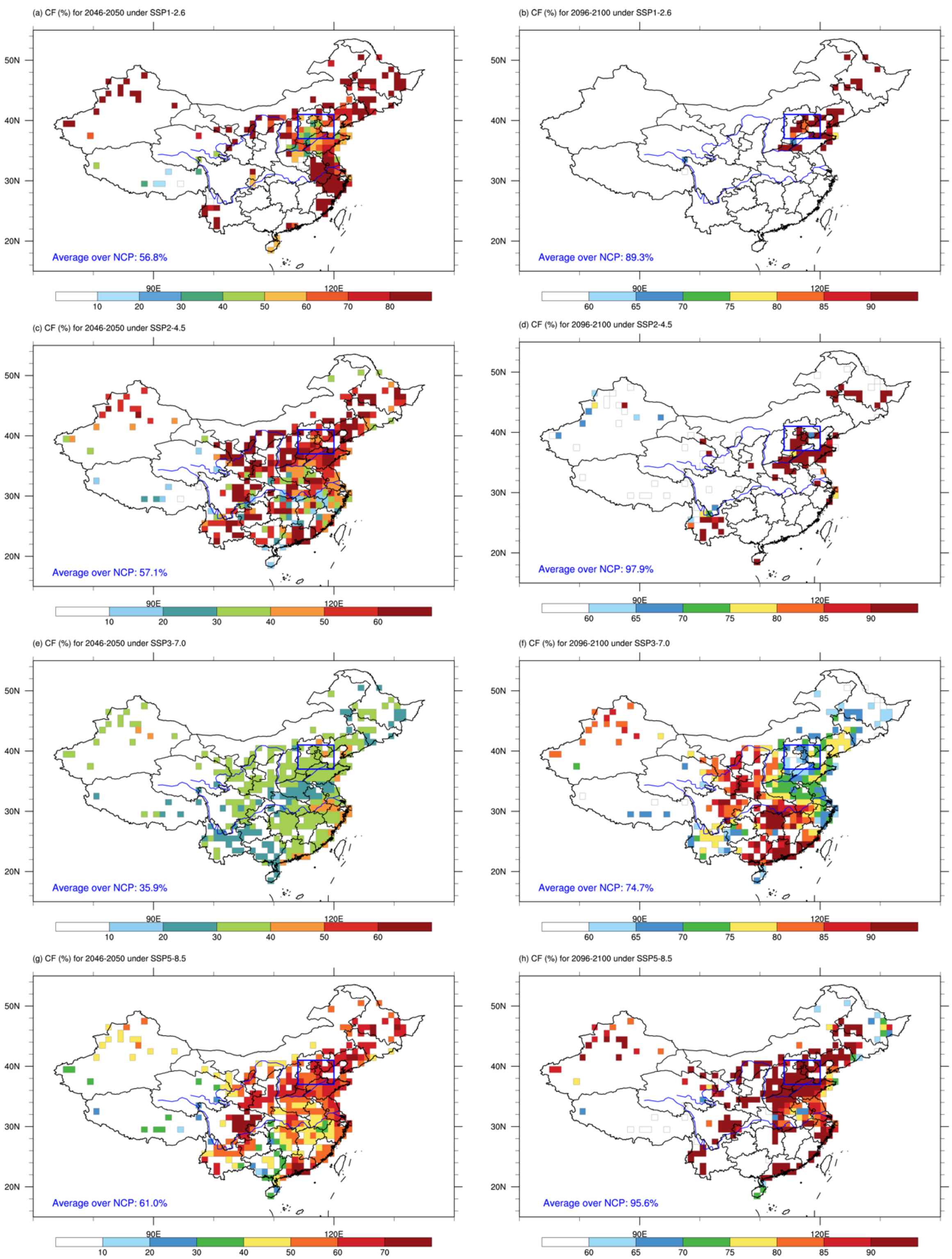

Figure S7. Same as Figure S6, but for CF values (%). CF values (%) averaged over NCP (37-41ºN; 114-120ºE) are indicated at the bottom left corner of each panel.

Table S1. Information of the CMIP6 models used in this study.

Model	Horizontal Resolution (Lon x Lat)	Time range	Institution
MOHC.UKESM1-0-LL	192 x 144	2015-2100	MOHC
CESM2-WACCM	288x 144	2015-2100	NCAR
GFDL-ESM4	288x180	2015-2100	NOAA-GFDL
MPI-ESM-1-2-HAM	192x96	2015-2055	HAMMOZ-Consortium
EC-Earth3-AerChem	120x90 for O_3 concentration 512x256 for temperature	2015-2100	EC-Earth-Consortium

Table S2 Models (ticked) providing simulations for each SSP scenario. Note that most of the adopted models provide hourly O_3 concentration and daily Tmax except the MOHC.UKESM1-0-LL simulations under SSP5-8.5 provide 3-hourly surface air temperature (Tas) and the GFDL-ESM4 simulations under SSP2-4.5 provide hourly Tas; thus, daily Tmax for the two GCMs are derived from hourly or 3-hourly Tas.

Model	SSP1-2.6	SSP2-4.5	SSP3-7.0	SSP5-8.5	Citation
MOHC.UKESM1-0-LL	√	√	√	√	Good et al. (2019)
CESM2-WACCM		√		√	Danabasoglu G (2019)
GFDL-ESM4		√			John et al. (2018)
MPI-ESM-1-2-HAM			√		Neubauer et al., 2019
EC-Earth3-AerChem			√		EC-Earth Consortium (EC-Earth) (2019)

References

Cheng, J., Tong, D., Liu, Y., Yu, S., Yan, L., Zheng, B., Geng, G., He, K., and Zhang, Q. J. G. R. L.: Comparison of current and future $PM_{2.5}$ air quality in China under CMIP6 and DPEC emission scenarios, 48, e2021GL093197, 2021.

Danabasoglu, G.: NCAR CESM2-WACCM model output prepared for CMIP6 ScenarioMIP. Earth System Grid Federation. https://doi.org/10.22033/ESGF/CMIP6.10026, 2019.

EC-Earth Consortium: EC-Earth-Consortium EC-Earth3-Veg model output prepared for CMIP6 ScenarioMIP. Earth System Grid Federation. https://doi. org/10.22033/ESGF/CMIP6.727, 2019.

EPA U: Guidance on the use of models and other analyses for demonstrating attainment of air quality goals for ozone, $PM_{2.5}$, and regional haze. US Environmental Protection Agency, Office of Air Quality Planning and Standards, 2007.

Good, P., Sellar, A., Tang, Y., Rumbold, S., Ellis, R., Kelley, D., Kuhlbrodt, T., Walton, J.: MOHC UKESM1.0-LL model output prepared for CMIP6 ScenarioMIP. Earth System Grid Federation. https://doi.org/10.22033/ESGF/CMIP6.1567, 2019.

John, J. G., Blanton, C., McHugh, C., Radhakrishnan, A., Rand, K., Vahlenkamp, H., Wilson, C., Zadeh, N. T., Dunne, J. P., Dussin, R., Horowitz, L. W., Krasting, J. P., Lin, P., Malyshev, S., Naik, V., Ploshay, J., Shevliakova, E., Silvers, L., Stock, C., Winton, M., Zeng, Y., NOAA-GFDL GFDL-ESM4 model output prepared for CMIP6 ScenarioMIP.Earth System Grid Federation. https://doi.org/10.22033/ESGF/CMIP6.1414, 2018.

Neubauer, D., Ferrachat, S., Siegenthaler-Le Drian, C., Stoll, J., Folini, D. S., Tegen, I., Wieners, K., Mauritsen, T., Stemmler, I., Barthel, S., Bey, I., Daskalakis, N., Heinold, B., Kokkola, H., Partridge, D., Rast, S., Schmidt, H., Schutgens, N., Stanelle, T., Stier, P., Watson-Parris, D., Lohmann, U.: HAMMOZ-Consortium MPI-ESM1.2-HAM model output prepared for CMIP6 AerChemMIP.Earth System Grid Federation. https://doi.org/10.22033/ESGF/CMIP6.1621, 2019.

Wang, Z., Lin, L., Xu, Y., Che, H., Zhang, X., Zhang, H., Dong, W., Wang, C., Gui, K., Xie, B. J. n. C., and Science, A.: Incorrect Asian aerosols affecting the attribution and projection of regional climate change in CMIP6 models, 4, 1-8, 2021.

Zhang, J., Gao, Y., Luo, K., Leung, L. R., Zhang, Y., Wang, K., Fan, J. J. A. C., and Physics: Impacts of compound extreme weather events on ozone in the present and future, 18, 9861-9877, 2018.